The Journal of Chemical Physics

The ground and ionized states of azulene: A combined study of the vibrational energy levels by photoionization, configuration interaction, and density functional calculations

Cite as: J. Chem. Phys. **156**, 064305 (2022); https://doi.org/10.1063/5.0073505
Submitted: 30 September 2021 • Accepted: 25 January 2022 • Accepted Manuscript Online: 25 January 2022 • Published Online: 11 February 2022

Michael H. Palmer, Marcello Coreno, Monica de Simone, et al.

The Journal of Chemical Physics ARTICLE scitation.org/journal/jcp

The ground and ionized states of azulene: A combined study of the vibrational energy levels by photoionization, configuration interaction, and density functional calculations

Cite as: J. Chem. Phys. 156, 064305 (2022); doi: 10.1063/5.0073505
Submitted: 30 September 2021 • Accepted: 25 January 2022 •
Published Online: 11 February 2022

Michael H. Palmer,[1,a] Marcello Coreno,[2,b] Monica de Simone,[3,c] Cesare Grazioli,[3,d] Nykola C. Jones,[4,e] Søren Vrønning Hoffmann,[4,f] and R. Alan Aitken[5,g]

AFFILIATIONS

[1] School of Chemistry, University of Edinburgh, Joseph Black Building, David Brewster Road, Edinburgh EH9 3FJ, Scotland, United Kingdom
[2] ISM-CNR, Instituto di Struttura della Materia, LD2 Unit, 34149 Trieste, Italy
[3] IOM-CNR, Istituto Officina dei Materiali, Basovizza SS-14, Km 163.5, 34149 Trieste, Italy
[4] ISA, Department of Physics and Astronomy, Aarhus University, Ny Munkegade 120, DK-8000 Aarhus C, Denmark
[5] School of Chemistry, University of St Andrews, North Haugh, Fife, St Andrews KY16 9ST, Scotland, United Kingdom

[a] **Author to whom correspondence should be addressed:** m.h.palmer@ed.ac.uk
[b] **Email:** marcello.coreno@elettra.eu
[c] **Email:** desimone@iom.cnr.it
[d] **Email:** grazioli@iom.cnr.it
[e] **Email:** nykj@phys.au.dk
[f] **Email:** vronning@phys.au.dk
[g] **Email:** raa@st-andrews.ac.uk

ABSTRACT

A synchrotron-based photoionization spectrum of azulene shows a significant additional vibrational fine structure when compared to previous studies. This spectrum was successfully analyzed by using Franck–Condon (FC) methods. Previously reported zero-kinetic-energy electron spectra for azulene have been reinterpreted in FC terms, leading to some alternative assignments to the earlier work. The sequence of ionic states has been determined by using *ab initio* configuration interaction (CI) methods, leading to reliable theoretical values for both the calculated adiabatic ionization energy (AIE) and vertical ionization energy (VIE). VIEs were calculated by both symmetry-adapted cluster (SAC-CI), together with Green's function (GF) and Tamm–Dancoff approximation (TDA), and single excitation CI methods; AIEs for highest states of each symmetry were determined by open-shell self-consistent field (SCF) methods at the restricted Hartree–Fock level. Complete active space SCF was used for the pairs of $1^2A_2 + 2^2A_2$ and $1^2B_1 + 2^2B_1$ states, each of which occurs as antisymmetric and symmetric (higher energy) combinations. The combined ionic state sequences (AIE and VIE) from these methods are $1^2A_2 < 1^2B_1 < 2^2A_2 < 2^2B_1$. The photoelectron spectrum (PES) shows a series of broadbands above 11 eV, each of which is attributed to more than one ionization. The calculated PES sequence of states of up to 19 eV shows that the SAC-CI and GF results are in almost exact agreement. The internal spacing of the bands is best reproduced by the simpler GF and TDA methods. States involving simultaneous ionization and electronic excitation are considered by both SAC-CI and TDA methods.

I. INTRODUCTION

Recently, we reported synchrotron-based high-resolution photoelectron spectrum (PES) and vacuum ultraviolet (VUV) absorption spectra for some highly conjugated molecules, including cyclooctatetraene (COT),[1,2] cycloheptatriene (CHT),[3,4] and norbornadiene (NBD).[5,6] Through-space interactions between non-bonded degenerate C=C π-bonds occur in these molecules.

We now report a new PES study of the fully conjugated molecule azulene (1) that is isomeric with naphthalene (2); both are shown in Fig. 1.[7–10] We demonstrate significantly higher spectral resolution than previously reported for 1.[11–13] The additional vibrational structure disclosed is analyzed by using Franck–Condon (FC) methods. Although both 1 and 2 are fully conjugated, azulene has some properties more like those of a deca-1,3,5,7-pentaene, where the C_9C_{10} bond is replaced by two H-atoms. The contrasts between 1 and 2 include color, where 1 is azure blue in color (hence the name), while 2 and most other hydrocarbons are colorless.

Microwave (MW) spectral studies of the ground X^1A_1 state of azulene show a planar structure with C_{2V} symmetry.[14,15] Gaseous 1 has a significant dipole moment (Fig. 1, DM),[14,15] in contrast to 2, which is nonpolar. The most accurate value for the azulene DM, shown in Fig. 1, is μ_A 0.8821 ± 0.0024 D, measured by microwave spectroscopy (MW);[9] values in solution are significantly higher. The azulene DM involves electron charge transfer from the seven- to the five-membered ring; the configuration in Fig. 1 shows full transfer of one-electron (δ = 1), whereby each ring effectively contains 6π-electrons, through sharing of those attributed to the C_9C_{10}-bond.[9]

These two compounds are classic alternant hydrocarbon (2, AH) and non-alternant hydrocarbon (1, NAH). In the AH series, the C-atoms can be marked by stars such that no two starred atoms are adjacent; this cannot be avoided in NAH systems owing to the odd-membered (5, 7) rings.

Eland and Danby (E & D)[11] performed the earliest PES and electron impact (EI) studies on azulene; the energetic results differ by up to 0.3 eV. The E & D PES gave a series of broad peaks, with vertical ionization energies (IEs) reported as follows: 7.42, 8.49, 9.91, and 10.81 eV; other than vertical ionization energies $(VIEs)_3$, these are effectively identical to the work of Boschi *et al.*,[12] who gave the following: VIE_3: 10.07 eV. In both these studies,[11,12] IE_4 close to 11 eV is not a true maximum. In contrast, we observe a sharp peak at 10.9 eV, followed by further poorly defined maxima up to 11.6 eV.

Weber *et al.*[13] generated a PES from azulene by resonant two-photon excitation at 293.17 and 282.3 nm; these wavelengths generate the third and fourth singlet excited states (S_3 and S_4), respectively. The most significant feature of these spectra is that the azulene cations are generated with a very large amount of vibrational energy, leading to largely featureless bands;[13] these are not directly comparable to the conventional PES.

The new PES vibrational results also allow us to reconsider assignments of earlier mass-selected ion-current spectra and zero-kinetic-energy (ZEKE) electron spectra by Tanaka *et al.*[16] These were performed for both azulene and its van der Waals complex with argon in a supersonic jet.[17] This also used two-photon (1 + 1′) resonant ionization via S_2. The adiabatic ionization energies (AIEs) for these two species are 59 781(5) cm^{-1} (7.4118 eV, 1) and 59 708(5) cm^{-1} (7.4027 eV, 1 + Ar), respectively,[16] showing a difference of only 73 cm^{-1}. The free azulene ZEKE spectrum showed a 0–0 band at the

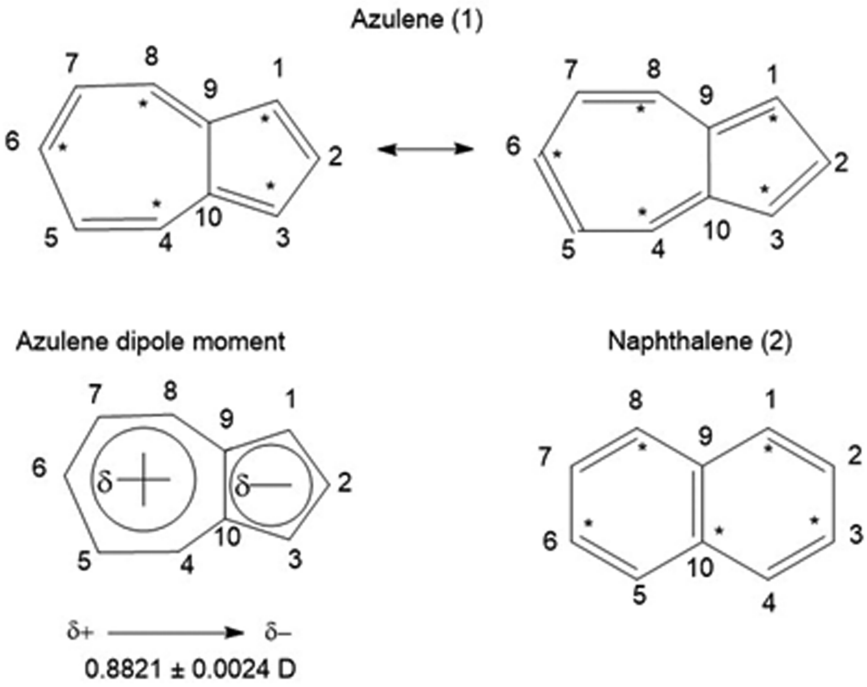

FIG. 1. Structures of azulene (1) and naphthalene (2).

S_2 origin, accompanied by several vibrational bands with frequencies as follows: 239, 373, 468, 661, 746, 886, and 918 cm^{-1}. The observed fundamental frequencies in the fluorescence spectra excited at the 236 and 468 cm^{-1} bands correspond to the ν_{39} (326 cm^{-1}) and ν_{38} (477 cm^{-1}) modes, respectively, both of b_1 symmetry. Similarly, the ν_{16} (a_1, 662) and ν_{37} (b_1, 668 cm^{-1}) bands in the absorption spectrum were thought to be active. Thus, in those studies, non-symmetric vibrations were proposed for some observed vibrations based on fluorescence spectra obtained by Fujii *et al.*,[17] from the S_2, S_3, and S_4 excited states to the ground state (S_0) of azulene. Modes 37, 38, and 39, vibrations of b_1 symmetry, were thought to arise from vibronic coupling. We will offer an alternative assignment involving fully symmetric bands below. In both these ZEKE and fluorescence studies, the labels b_1 and b_2 for vibrational modes are interchanged relative to the present study;[18] both conventions lead to identical numerical results and are a result of different coordinate systems being used for the molecule.

This paper discusses the ionic states of azulene determined by both PES and ZEKE; similar discussion of the ground and corresponding singlet and triplet state manifolds is deferred to a later paper. Our experimental results are interpreted by high-level theoretical studies, including symmetry adapted cluster configuration interaction (SAC-CI), complete active space SCF (CASSCF), and CI calculations. We perform Franck–Condon vibrational state analyses of our new synchrotron-based PES using the Pisa group software[19–21] incorporated in Gaussian-16 (G-16),[22] where processing of the vibrational analysis is limited to a single imaginary frequency. Some highly bound ionic states generate imaginary frequencies, implying that the structures are saddle points rather than genuine minima.

II. METHODS

The azulene sample, complete active space (CAS) registry number 275-51-4, purchased from Sigma-Aldrich (product number A97203, 99% purity), was used without further purification.

A. The UV-photoelectron spectrum of azulene

This was obtained at room temperature on the gas-phase line of the Elettra synchrotron (Basovizza, near Trieste, Italy) using methods described previously.[1,3] The azulene vapor was irradiated with both 30 and 40 eV photon energies. The 30 eV spectrum covers the energy range of 7.057–14.257 eV with 4571 data points (DPs), separated by 0.001 eV (8 cm^{-1}) up to 9.357 eV, with 0.002 eV separation at higher energy. A wider scan of up to 19.180 eV, using 40 eV irradiation, contained 1251 DPs, with a separation of 0.01 eV.

The 30 eV spectrum corresponds to an overall resolution close to 8.5 meV; we adopt a conventional definition of resolution as the minimum separation between two lines where it is possible to distinguish between them. The precision of the measured energies and the resolution were also determined from argon PES lines, which are known from the literature. Ar is added to the sample as an additional calibrant.

The absolute positions of the principal PES bands, determined by the program Multi-peak Fit (Version 2.22), are shown in Fig. 2 and Table I; additional peak-fit statistics are shown in the supplementary material as SM1. The peak separations shown in Table I are relevant to the Franck–Condon separations determined theoretically below. Previous vibrational separations reported by Boschi *et al.*[12] for the lowest ionization of azulene are 830, 1130, 1340, and 1990 cm^{-1}, where all are ±70 cm^{-1}; the values in Table I are consistent with these earlier results, although ours have a smaller uncertainty.

B. Theoretical methods

Several computational chemistry suites were used since none offers us a complete analysis. The equilibrium structures for the X^1A_1 ground state and several of the lowest ionic states of each symmetry were determined by (restricted) open shell Hartree–Fock (RHF) calculations using the G-16 suite.[22]

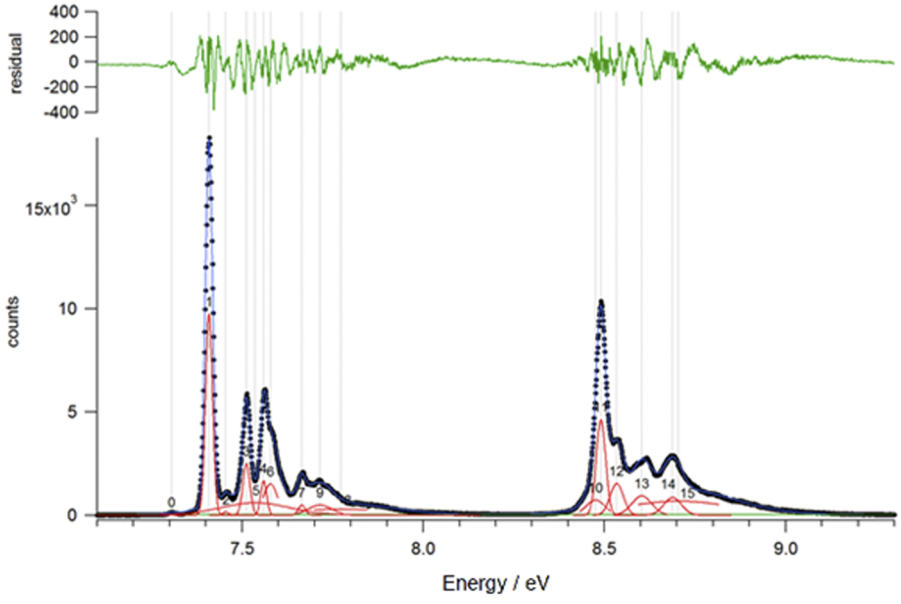

FIG. 2. Location of peak maxima for bands A and B. There is evidence of a hot-band at the onset to band B. Peaks 1–15 (red) are individual fits to peaks observed, as listed in Table I; residuals are shown in green above. These represent a very small proportion of the overall PES counts shown. The red peaks shown indicate position only, and their intensities are scaled to fit, leaving the residuals shown.

TABLE I. Peak positions from the multi-peak analysis; errors in the last digit shown are in parentheses.

Band A				Band B			
Peak label	Location (cm^{-1})	Location (cm^{-1})	Peak separation (cm^{-1})	Peak label	Location (cm^{-1})	Location (cm^{-1})	Peak separation (cm^{-1})
P0	7.305(2)	58 920	0	P10	8.47(5)	68 316	−165
P1	7.409(1)	59 758	838	P11	8.490(1)	68 481	0
P2	7.455(1)	60 130	1210	P12	8.534(1)	68 833	352
P3	7.512(1)	60 590	1670	P13	8.603(1)	69 388	907
P4	7.560(1)	60 975	2055	P14	8.688(1)	70 073	1592
P5	7.536(5)	60 981	2061	P15	8.70(1)	70 204	1723
P6	7.578(5)	61 126	2206				
P7	7.665(1)	61 823	2903				
P8	7.77(2)	62 670	3750				
P9	7.715(1)	62 225	3305				

Several density functional theory (DFT) functionals[23] were tested, including the Becke + (three-parameter) Lee–Yang–Parr (B3LYP) hybrid functional.[24] Overall, a long-range-corrected version of B3LYP, the Coulomb-attenuating method (CAM-B3LYP),[25] proved to give the best results; this was in terms of energy separations between ionic states and also in terms of balance between the 0–0 band and vibrational satellite intensities determined by the Pisa software discussed below. A double hybrid method, B2PLYPD3, combining a Møller–Plesset type of correlation within a DFT calculation, gave good adiabatic ionization energies (AIEs),[26–28] but a very high proportion of the intensity was concentrated in the 0–0 band and a very much lower intensity for the fundamentals and combination bands. This contrasts with the PES spectral profile.

The RHF-method incorporating the CAM-B3LYP procedure was only applicable to the lowest ionic state of each symmetry. To determine the AIE for higher members of these manifolds, complete active space self-consistent field (CASSCF) calculations were performed for the pairs of $1^2A_2 + 2^2A_2$ and $1^2B_1 + 2^2B_1$ states using G-16.[22] These calculations included seven-electrons permuted into eight-molecular orbitals (MOs), conventionally termed CASSCF [7,8], and generated 3920 configurations. The higher energy states, 2^2A_2 and 2^2B_1, proceeded normally using this method[22] by choice of the second root for optimization in two-root searches. These CASSCF calculations generated linear combinations of states, such as $1^2A_2 \pm 2^2A_2$. All these RHF and CASSCF calculations gave wave-functions, which were input to the Pisa software as described below.

Although a more general solution to this problem would be the use of the MCSCF package in the MOLPRO suite,[29] where both the root and the symmetry are selected, this package does not produce output, which is currently acceptable to our version of the Pisa software. Some MOLPRO results for structures of higher roots are shown in the supplementary material as SM2.

C. Basis sets

Modern bases deliberately contain a wide range of exponents, which cater for both valence and Rydberg state determination. Ionic states strongly require valence shell functions. Such Gaussian-type orbitals (GTOs) are present in various older basis sets, such as 6-311G(d,p),[30,31] otherwise known as 6-311G,** which is used in the main thrust of this work.

III. RESULTS

A. Structures

Microwave spectroscopy shows that the molecular structure of azulene is a relatively rigid molecule[14,18] with rotational constants (RCs) A = 2841.951(24), B = 1254.846 34(10), and C = 870.7162(8) MHz.[14] The RCs for the equilibrium structure of azulene using the 6-311G(d,p) basis set in the RHF method are very similar to the following: A = 2876.87, B = 1265.89, and C = 879.08 MHz. This basis is also used for all the ionic state structures undergoing analysis, namely, the 1^2A_2, 1^2B_1, 2^2A_2, 2^2B_1, and 1^2A_1 states. Since equilibrium structures are not the focus of this paper, they are shown in the supplementary material as SM3. The vibrational structure for each of these states is discussed below.

B. Assignment of the wide scan azulene photoelectron spectrum from 6.5 to 19 eV

The wide PES scan measured with 40 eV photon irradiation is shown in Fig. 3, with bands designated as A to M for simplicity, although some, such as D + E, F + G, and H + I, contain overlapping members. Only three bands A, B, and D show a well-defined vibrational structure, as discussed below. In the following sections, we present new assignments for (a) the vertical ionization energies (VIEs) of numerous valence shell ionic states, together with their relative intensities, and (b) adiabatic excitation energies (AIEs) together with their vibrational structure, which will be analyzed by using Franck–Condon methods.

The most intense PES bands are often denoted as Koopmans' theorem (KT) bands; these are where almost all the intensity of the band is represented by a one-electron (1e) process; for example, the highest occupied molecular orbital ($2a_2^2$) has a single electron removed, generating $2a_2^{-1}$; in KT processes involving this MO, this configuration is dominant, and the energy of the KT state is close

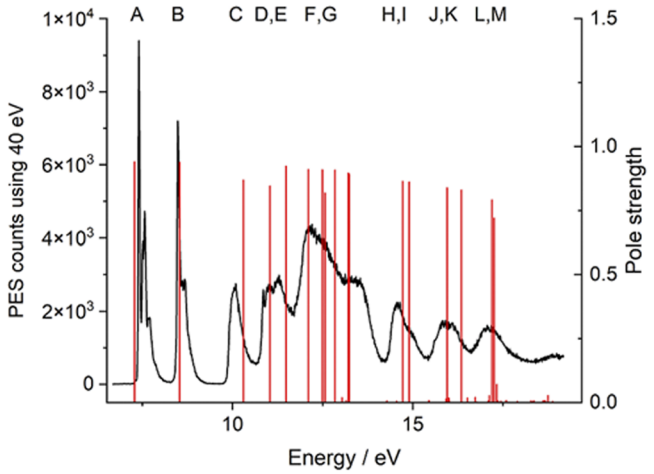

FIG. 3. The wide scan photoelectron spectrum (PES) of azulene using 40 eV irradiation (black curve) with the SAC-CI monopole strengths (red lines). The principal bands of the PES have been labeled A to M for ease of description in the text. The energies (eV) have been scaled using the following equation: VIE_{pes} = 0.90 * VIE_{calc} + 1.30. A set of well-defined IEs were chosen. The energies of the calculated peaks closest to these ionizations were then plotted against the measured set, establishing a correlation line. All the calculated energies were then scaled by that correlation equation. The same applies for Fig. 4.

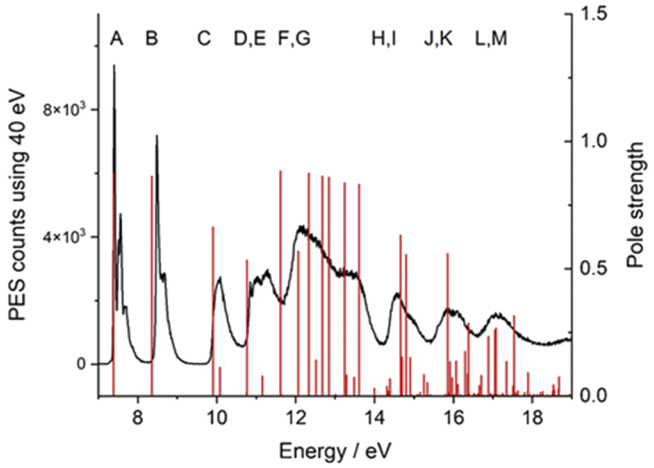

FIG. 4. The wide scan photoelectron spectrum (PES) of azulene using 40 eV irradiation (black curve), with the TDA monopole strengths (red lines). The principal bands of the PES have been labeled A to M for ease of description in the text. The energies (eV) have been scaled to fit the spectral range using the following equation: VIE_{pes} = 0.875 * VIE_{calc} + 1.368.

to the occupied orbital energy for that configuration. Structural relaxation in the ion is variable, but it can be substantial, with consequential lowering of the energy. Many weaker bands are also present, where ionization is accompanied by electronic excitation; these are two-electron (2e) processes, widely known as shake-up states. We present theoretical results for both 1e- and 2e-states, including ionic state energies (eV) and their intensities (pole strengths).

We assign the overall PES envelope over the range shown in Fig. 3, utilizing several methods; (a) our most rigorous level used the symmetry-adapted coupled cluster method developed by Nakatsuji *et al.* (SAC-CI),[32–36] as installed in G-16.[22] (b) In contrast, Green's function (GF) method for 1e processes only and Tamm–Dancoff approximation (TDA), which includes 2e-processes, both single excitation CI[37–39] methods, are implemented in GAMESS-UK.[40]

The theoretical manifold shown in Fig. 3 uses the SAC-CI model. Above 12 eV, several very weak lines are apparent, which are 2e-processes. In general, the SAC-CI method gives a good account of the PES profile, but with the onset peaks and those near17 eV being used for the range of the PES fit, the peaks near the center of the PES, from 10 to 13 eV, especially for IE_3 and IE_{4+5}, do not give close fits. The active MOs used in the SAC-CI calculations are of the full valence shell range.

The TDA results in Fig. 4 give a much closer fit for $IE_{3,4,5}$; this also shows the 2e-processes more dramatically; their simplicity in calculation and interpretation makes these the choice in the current study. The high energy range close to 20 eV is uneven in the TDA theoretical intensities; this arises from the physical limits imposed on the range of active MOs (20 for each representation) in the TDA code. Thus, some excitations that are necessary for a smooth curve are excluded. GF is presented in the supplementary material as SM4; its results are similar to both the SAC-CI and TDA, but the decline in pole strengths with energies seems delayed relative to the PES experiment.

Deleuze *et al.*[41] reported theoretical PES of azulene using a third-order algebraic diagrammatic construction [ADC (3)] scheme similar to TDA. They suggested that two 2e-processes occur after the second ionization band (B), with energies close to 9.6 and 10.6 eV. The present onset for 2e-processes using the TDA method is higher energy at 10.08 and 11.20 eV. The calculations of Deleuze *et al.*[41] used both a low resolution PES and theoretical linewidths, denoted by Full Width at Half Maximum (FWHM) of 0.5–1.0 eV. In our fits below, we use FWHM down to 10 cm^{-1}, and hence show much more detail, and also with a more balanced aspect ratio.

The principal numerical 1e-results of the open-shell CI calculations by SAC-CI and Green's function methods are shown in Table II. The SAC-CI VIEs are lower by 0.248 eV on average; this makes VIE_3 and VIE_4 difficult to correlate with the experiment. The first change of VIE between the methods occurs above 18 eV, with $10a_1$ and $7b_2$, the same position where the 1e-processes collapse with the onset of a dense 2e-profile. The results depicted in Table II show a considerable similarity in the VIE using either SAC-CI or GF methods over 17 valence MOs, with a linear correlation: VIE_{GF} = 0.996(8) * VIE_{SACCI} + 0.248(110). The correlation coefficient (adjacent R^2) is 0.9989, and standard errors are in parentheses. The two sets of results are effectively identical for 1e-processes; this level of agreement is unexpected and very satisfactory. The GF and TDA single excitation CI method calculations are dramatically shorter in processor time than the SAC-CI, a coupled cluster procedure. The computational cost of SAC-CI is larger by an order of magnitude, and this is likely to be its main limitation at present.

For all VIE below 17 eV, the calculated 1e-pole strengths are generally in the range of 0.7–0.9 and close to the limiting value of 1.0; at higher energy, a rapid drop to zero occurs. Up to this limit, it is reasonable to use MO electron 1e-vacancies interchangeably with

TABLE II. The vertical ionization energies for azulene. (a) Symmetry adapted cluster configuration interaction (SAC-CI) and (b) Greens' function third order perturbation theory. All electron numbering is used to assist comparison with earlier studies. These are the theoretical results, which have been scaled to fit in the correlation with the experimental PES discussed below. The first difference in the ionic state sequences occurs with $10a_1$ and $7b_2$ at 17.851 and 20.538 eV, respectively π-electron orbitals vacated and their corresponding ionic states are shown in bold.

	SAC-CI		Green's function		
Orbital vacated	Energy (eV)	Monopole strength	Energy (eV)	Monopole strength	State
$2a_2$	6.646	0.940	7.040	0.888	**1^2A_2**
$3b_1$	7.921	0.938	8.165	0.887	**1^2B_1**
$1a_2$	9.996	0.869	10.133	0.827	**2^2A_2**
$2b_1$	10.789	0.846	11.008	0.780	**2^2B_1**
$17a_1$	11.316	0.923	11.428	0.895	1^2A_1
$12b_2$	12.076	0.910	12.164	0.886	1^2B_2
$1b_1$	12.522	0.818	12.765	0.780	**3^2B_1**
$11b_2$	12.527	0.908	12.871	0.885	2^2B_2
$16a_1$	12.619	0.908	12.643	0.885	2^2A_1
$15a_1$	13.167	0.892	13.304	0.871	3^2A_1
$10b_2$	13.419	0.896	13.643	0.870	3^2B_2
$9b_2$	14.861	0.863	15.025	0.856	4^2B_2
$14a_1$	14.974	0.861	15.159	0.844	4^2A_1
$13a_1$	16.117	0.838	16.354	0.835	5^2A_1
$8b_2$	16.605	0.830	16.699	0.801	5^2B_2
$12a_1$	17.529	0.791	17.762	0.790	6^2A_1
$11a_1$	17.714	0.720	18.070	0.674	7^2A_1

1e-states, even though considerable electron reorganization between the neutral and ionic states would have occurred; thus, $2a_2{}^{-1}$ is a good representation of 1^2A_2. This correlation between orbitals and states breaks down when "shake-up" states occur.

Within states of the same symmetry, there is a trend for the pole strength to decline with an increase in binding energy. This is particularly striking with the $1b_1$ and $2b_1$ states, which have lower values than $3b_1$; a similar change occurs for $2a_2$ over $1a_2$.

The lowest calculated ionic state energies have the following sequence: $1^2A_2 < 1^2B_1 < 2^2A_2 < 2^2B_1 < 1^2A_1 < 1^2B_2$, with SAC-CI, GF, and TDA methods. Boschi *et al.*[12] gave the same sequence for the lowest four IEs, but their energy values are significantly different from ours. Their onset for the σ-IE sequence starts at 11.0 eV; this would be associated with our 3^2B_1 ionization. Early *ab initio* calculations on naphthalene and azulene by Buenker and Peyerimhoff[42] drew attention to the intermingling of $\pi-$ and $\sigma-$ levels in their occupied orbitals, with ascending sequences of energy, based on orbital energies, with azulene: π, π, π, π, σ, σ, π and naphthalene: π, π, π, π, σ, σ, σ, π.

C. Vibrational structure shown in the PES bands

The following sections represent the first detailed analysis of the vibrational structure of the azulene PES. All orbitals and electrons are included in our computations, but we use valence shell numbering for the occupied molecular orbital (MO) and virtual molecular orbital (VMO) to facilitate a comparison with other work.

In the Franck–Condon results shown in the Tables III–VIII, the molar absorption coefficient intensities are $dm^3\ mol^{-1}\ cm^{-1}$. The 48 fundamental modes of azulene in C_{2v} symmetry are $17a_1 + 6a_2 + 9b_1 + 16b_2$. Those of a_1 and b_2 symmetry correspond to in-plane vibrations, while those of a_2 and b_1 symmetry are out-of-plane deformations. In conventional infrared spectroscopy, modes are sequenced $a_1 < a_2 < b_1 < b_2$; these are given as a_1: 1–17, a_2: 18–23, b_1: 24–32, and b_2: 33–48. However, the Franck–Condon analyses using the Pisa suite follow the G-16 convention of labeling modes from lowest to highest frequency, irrespective of symmetry. In the more conventional spectroscopic notation, the highest is $1a_1$ and goes via a_2 and b_1 to the lowest $16b_2$. For simplicity and to avoid errors, we refer to prominent fundamentals present in the calculated envelopes by the calculated frequency using the Gaussian-16 labels. It is important to note that the ZEKE and fluorescence studies discussed below do not adhere to the standard sequence for vibrational frequencies by state, as above. They use the following: a1: 1–17, a_2: 18–23, b_1: 24–39, and b_2: 40–48. Thus, our discussion of the ZEKE spectrum adopts their sequence to maintain backward compatibility. Full sets of harmonic frequencies for each electronic state studied, including the X^1A_1 ground state, are shown in the supplementary material as SM5. A full list of a_1 symmetry frequencies, determined with the CAM-B3LYP method and the 6-311G(d,p) basis set, is shown in Table III; these are used in the Franck–Condon (FC) analyses.

TABLE III. The CAM-B3LYP calculated a_1 symmetry harmonic frequencies, rounded to integral cm^{-1} values, used in the Franck–Condon (FC) analyses for the ionic states of azulene. In FC states, only a_1 modes are active. In Gaussian-16, these have sequential numbering from the lowest (mode 1) to highest frequency (mode 48). The Pisa Group software, internal to G-16, continues this system. This numbering differs from the standard system used in vibrational spectroscopy. The position of the a_1 modes in the overall C_{2V} sequence varies with the electronic state. The sequence numbers in parentheses ({}) are those used in the FC analyses shown in Table IV onward.

	State					
FC mode	X^1A_1	1^2A_2	1^2B_1	2^2A_2	2^2B_1	1^2A_1
1	415{5}	410{6}	406{6}	423{6}	414{7}	320{5}
2	692{10}	696{10}	670{10}	709{11}	687{10}	465{7}
3	845{16}	859{15}	830{16}	883{16}	882{13}	730{12}
4	924{18}	911{17}	913{18}	968{20}	918{15}	866{15}
5	978{21}	974{19}	951{19}	1011{22}	966{16}	965{18}
6	1093{26}	1114{26}	1053{22}	1167{26}	1095{23}	1087{24}
7	1257{29}	1255{28}	1264{29}	1280{28}	1334{29}	1136{26}
8	1322{30}	1275{30}	1305{30}	1315{29}	1364{30}	1256{29}
9	1447{34}	1452{34}	1431{33}	1530{34}	1519{33}	1314{30}
10	1512{36}	1515{37}	1510{35}	1612{36}	1575{35}	1502{34}
11	1611{38}	1619{38}	1589{37}	1667{37}	1637{35}	1609{36}
12	1679{40}	1635{39}	1682{39}	1731{38}	1750{39}	1679{38}
13	3155{41}	3186{41}	3183{41}	3336{40}	3341{41}	3008{40}
14	3165{43}	3195{43}	3190{43}	3343{42}	3356{43}	3183{42}
15	3193{45}	3211{45}	3215{45}	3370{44}	3372{45}	3191{43}
16	3217{46}	3241{46}	3238{46}	3383{45}	3390{46}	3223{45}
17	3244{48}	3265{48}	3266{48}	3404{47}	3408{48}	3263{46}

1. Band A: The $^2A_2$ state

The high resolution structure of the lowest ionized state, the 1^2A_2 state, is shown in Fig. 5, with the detailed vibrational bands from Table IV superimposed. The most detailed previous interpretation[12] for this state was in terms of four vibrations, as 830, 1130, 1340, and 1990 cm^{-1}, but with a significant degree of uncertainty (±70 cm^{-1}).[12] The two lowest values are relatively close to the present calculated ones for modes 15 and 26 (859 and 1114 cm^{-1}), but our strongest contributor, mode 30, is rather different at 1275 cm^{-1}. We have no fundamental close to 1990 cm^{-1}, but a series of peaks occuring, starting near 61 750 $cm^{-1}$and shown in Fig. 5, could have led to this interpretation. The same overtones and binary combination bands, shown in Table IV, 1718 cm^{-1} (15^2), 2115 cm^{-1} (28^1; 15^1), and 2134 cm^{-1} (30^1; 15^1), etc., have frequencies in this region. Modes 6, 10, 15, 19, 26, 28, 30, and 34 all occur in the description of the 1^2A_2 state.

2. Band B. The 1^2B_1 state, close to 8.5 eV

The dominant fundamentals for band B contain major contributions from modes 6, 10, 19, 22, 29, 35, and 39, especially in the combination bands shown in Table V; most of the band A fundamentals are not present in band B. Thus, the superficial similarity in the structure between bands A and B, as shown in Figs. 5 and 6, is accidental, and the two are different in character.

3. Band C, the 2^2A_2 state close to 10 eV

The analysis is dominated by modes 6, 11, 16, 22, 28, 34, and 37, but with large differences in intensity, as shown in Table VI; a short sequence in mode 6^n (n = 1, 2, 3) occurs, but most of Table VI

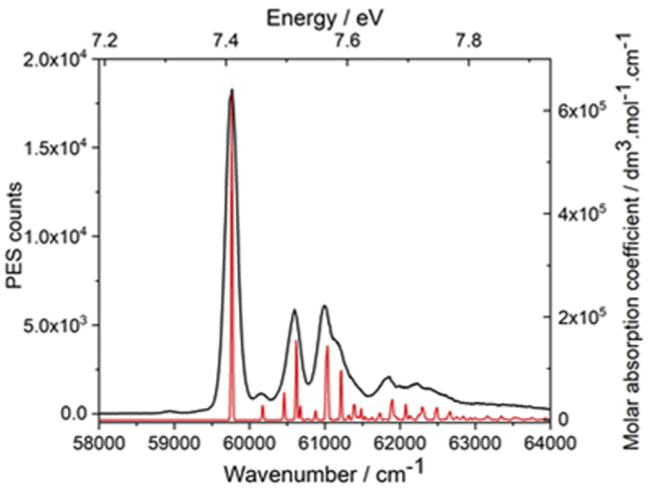

FIG. 5. Azulene $^2A_2$ ionic state (black curve) with the CAM-B3LYP functional superimposed (red). The theoretical spectrum energy has been increased by 2230 cm^{-1} to overlay the experimental spectrum. The B2PLYPD3 functional gives a closer fit to the experimental AIE (energy shift only 811 cm^{-1}), but the cross section of the theoretical spectrum is almost entirely localized (99%) in the 0–0 band.

TABLE IV. Calculated energy levels, using the CAM-B3LYP method, and intensities for the 1^2A_2 ionic state of azulene. All active fundamentals and other overtones; combination bands shown are based on highest intensity. Calculated energy of the 0–0 (0^0) transition: 57 610 cm^{-1} (7.1425 eV).

Energy (cm^{-1})	Excitation	Intensity	Energy (cm^{-1})	Excitation	Intensity
0	0^0	632 900	1619	38^1	21 990
316	1^2	151	1635	39^1	23 330
318	2^2	433	1666	$28^1; 6^1$	4 784
410	6^1	28 790	1685	$30^1; 6^1$	4 668
607	3^2	240	1718	15^2	17 610
696	10^1	53 630	1770	$17^1; 15^1$	7 167
775	5^2	825	1811	$26^1; 10^1$	1 380
821	6^2	466	1863	$34^1; 6^1$	3 458
859	15^1	154 900	1952	$28^1; 10^1$	4 549
879	$11^1; 1^1$	1 245	1971	$30^1; 10^1$	7 791
911	17^1	20 160	2115	$28^1; 15^1$	27 220
974	19^1	167	2134	$30^1; 15^1$	28 120
1007	7^2	1 779	2166	$28^1; 17^1$	4 536
1107	$10^1; 6^1$	1 659	2186	$30^1; 17^1$	5 339
1114	26^1	16 900	2311	$34^1; 15^1$	19 660
1153	9^2	496	2332	$39^1; 10^1$	1 961
1255	28^1	77 320	2363	$34^1; 17^1$	4 974
1269	$15^1; 6^1$	6 718	2370	$28^1; 26^1$	2 967
1275	30^1	119 600	2390	$30^1; 26^1$	2 875
1321	$17^1; 6^1$	1 302	2478	$38^1; 15^1$	6 281
1393	10^2	2 097	2511	28^2	5 460
1452	34^1	92 900	2530	$30^1; 28^1$	19 170
1515	37^1	645	2708	$34^1; 28^1$	13 940
1555	$15^1; 10^1$	9 976	2727	$34^1; 30^1$	14 430
1607	$17^1; 10^1$	2 024			

TABLE V. Prominent theoretical Franck–Condon bands for band B, attributed to the 1^2B_1 state, based on CAM-B3LYP calculations.

Energy (cm^{-1})	Excitation	Intensity	Energy (cm^{-1})	Excitation	Intensity
0	0	654 900	1583	$18^1; 10^1$	2 228
274	1^2	4 548	1589	37^1	77 220
406	6^1	122 100	1670	$29^1; 6^1$	2 871
670	10^1	47 900	1682	39^1	171 100
811	6^2	14 930	1723	$22^1; 10^1$	14 880
830	16^1	30 250	1837	$33^1; 6^1$	2 882
913	18^1	35 500	1883	$22^1; 16^1$	10 130
951	19^1	4 049	1966	$22^1; 18^1$	6 343
955	7^2	5 294	1994	$37^1; 6^1$	21 710
1053	22^1	136 700	2088	$39^1; 6^1$	28 760
1076	$10^1; 6^1$	12 260	2105	22^2	15 390
1236	$16^1; 6^1$	8 161	2512	$39^1; 16^1$	11 370
1264	29^1	17 010	2641	$37^1; 22^1$	19 090
1319	$18^1; 6^1$	5 710	2734	$39^1; 22^1$	31 620
1458	$22^1; 6^1$	37 700	3271	$39^1; 37^1$	17 990
1510	35^1	14 040	3364	39^2	22 080

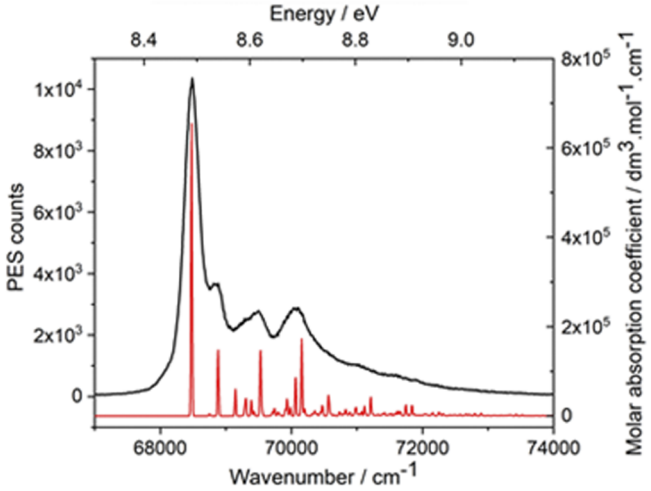

FIG. 6. Azulene $^2B_1$ PES state (black curve) using the CAM-B3LYP functional with the Franck–Condon profile superimposed (red).

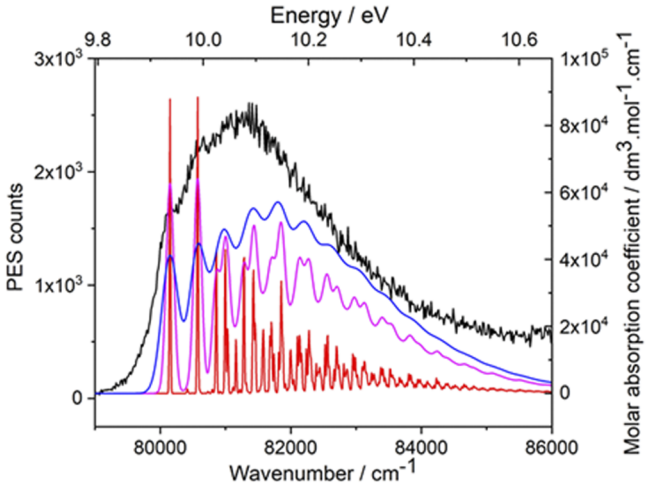

FIG. 7. Azulene PES band C (black curve) with the CASSCF 2^2A_2 state Franck–Condon envelope. The theoretical levels show sets of vibrational peaks corresponding to half-widths at half-maximum of 10 cm^{-1} (red), 70 cm^{-1} (magenta), and 150 cm^{-1} (blue).

is binary combinations of these, especially with the lowest frequency mode 6. Strong ternary combination bands are more prominent in intensity than for the other ionic states. The band, shown in Fig. 7, is comparatively narrow, but with a high 0–0 level.

TABLE VI. Band C assigned to the 2^2A_2 state, determined by CASSCF calculations: the most intense Franck–Condon bands.

Energy (cm^{-1})	Excitation	Intensity	Energy (cm^{-1})	Excitation	Intensity
0	0	87 870	1720	$22^1; 11^1$	4906
423	6^1	63 430	1729	$16^1; 6^2$	9433
709	11^1	37 390	1857	$22^1; 6^2$	7456
846	6^2	34 340	1978	$11^1; 6^3$	6543
883	16^1	18 360	2015	$16^1; 11^1; 6^1$	5848
1011	22^1	15 360	2143	$22^1; 11^1; 6^1$	5161
1132	$11^1; 6^1$	39 520	2163	$28^1; 16^1$	5487
1269	6^3	11 920	2239	$34^1; 11^1$	5404
1280	28^1	30 120	2264	$11^2; 6^2$	4956
1306	$16^1; 6^1$	18 980	2291	$28^1; 22^1$	4502
1418	11^2	10 490	2376	$34^1; 6^2$	5130
1434	$22^1; 6^1$	15 440	2377	$37^1; 11^1$	6054
1530	34^1	16 270	2513	$37^1; 6^2$	6462
1555	$11^1; 6^2$	20 090	2561	28^2	4576
1667	37^1	11 330	2586	$28^1; 16^1; 6^1$	5672
1703	$28^1; 6^1$	21 100	2662	$34^1; 11^1; 6^1$	5644
1841	$11^2; 6^1$	10 400	2714	$28^1; 22^1; 6^1$	4516
1953	$34^1; 6^1$	16 240	2810	$34^1; 28^1$	4694
1989	$28^1; 11^1$	11 150	2835	$28^1; 11^1; 6^2$	5989
2090	$37^1; 6^1$	12 330	2861	$16^1; 11^1; 6^3$	1012
2126	$28^1; 6^2$	11 440	3233	$34^1; 28^1; 6^1$	4677
2412	$28^1; 11^1; 6^1$	11 780	3371	$37^1; 28^1; 6^1$	4423

4. Bands D and E. An overlapping set of peaks assigned to the 2^2B_1 and 1^2A_1 ionic states

We note that a sharp peak occurs at 10.865 eV (87 631 cm^{-1}), which is out of character with other nearby peaks. We assign this

TABLE VII. The 1^2A_1 state, calculated by the CAM-B3LYP method, as onset to the combined bands D and E. The highest intensity bands lie nearly 0.5 eV higher in energy and are shown in the supplementary material as SM6. 0–0 band: 85 967 cm^{-1}.

Energy (cm^{-1})	Excitation	Intensity	Energy (cm^{-1})	Excitation	Intensity
0	0	305	1394	$7^2; 2^2$	89
320	5^1	370	1395	7^3	9583
465	7^1	1828	1406	$24^1; 5^1$	130
640	5^2	242	1424	$7^1; 5^3$	274
785	$7^1; 5^1$	3071	1429	$18^1; 7^1$	1059
866	15^1	37	1456	$26^1; 5^1$	850
929	$7^1; 2^2$	31	1502	34^1	40
930	7^2	5244	1506	$15^1; 5^2$	54
960	5^3	54	1511	$7^2; 3^2$	37
965	18^1	191	1552	$24^1; 7^1$	384
1087	24^1	73	1569	$7^2; 5^2$	3687
1105	$7^1; 5^2$	1699	1576	$29^1; 5^1$	206
1136	26^1	488	1601	$26^1; 7^1$	2794
1186	$15^1; 5^1$	75	1604	$18^1; 5^2$	207
1249	$7^1; 5^1; 2^2$	52	1609	36^1	35
1250	$7^2; 5^1$	7906	1639	$8^1; 7^2; 2^1$	27
1256	29^1	115	1645	$7^2; 6^1; 3^1$	40
1284	$18^1; 5^1$	341	1651	$15^1; 7^1; 5^1$	398
1331	$15^1; 7^1$	215	1659	$12^1; 7^2$	32
1366	$7^1; 5^1; 3^2$	24	1680	$20^1; 7^1; 2^1$	31

band D peak to the onset of 2^2B_1 ($2b_1^{-1}$); this calculated state has a sharp 0–0 peak. In contrast, the profile for 1^2A_1 has a low onset cross section, as shown in Table VII, and differs fundamentally from 2^2B_1.

After projection of the imaginary frequency and renumbering to account for this, the 1^2A_1 state shows the fundamentals 5, 7, 15, 18, 24, 26, 29, 34, and 36; these correspond to the following frequencies: 320, 465, 866, 965, 1087, 1136, 1256, 1502, and 1609, respectively. The principal components of the Franck–Condon analysis for the 2^2B_1 ionic state are shown in Table VIII and Fig. 8. The positioning of the higher component, the 1^2A_1 ionic state, shown in Table VII is uncertain, and here, it is chosen to correspond to the highest part of the intensity envelope close to 11.4 eV. The positioning of the 2^2B_1 state, with its high intensity 0–0 band, is natural, as shown in Fig. 9. In addition to the 0–0 band, the prominent modes are 7, 10, 14, 16, 22, 29, 30, 33, 37, and 39.

5. Comparison of the $^2A_2$ theoretical Franck-Condon envelope with the ZEKE spectrum

We note that Tanaka *et al.*[16] correlated fundamental vibrations for various electronically excited and ionic electronic states with neutral ground state vibrations in their ZEKE study. There is an implicit assumption that the sequence of frequencies exhibited is the same by symmetry. In the ZEKE study, the mass-selected ion-current spectrum obtained for neutral azulene, with the 0–0 band at 28 758 cm^{-1}, is accompanied by vibrational peaks at higher frequencies: 239, 373, 468, 661, 746, 886, and 918 cm^{-1}. These frequencies are very similar to those in the previously observed fluorescence excitation spectrum of the S_2 singlet state by Fujii *et al.*[17] This resonance Raman study adopted the notation of Chao and Khanna,[18]

TABLE VIII. Onset of the 2^2B_1 state, calculated by the CASSCF method. Energy of the 0–0 transition: 86 290 cm^{-1}.

Energy (cm^{-1})	Excitation	Intensity	Energy (cm^{-1})	Excitation	Intensity
0	0	340 500	811	$7^1; 4^1; 1^1$	1 270
147	1^2	32 620	814	$7^1; 2^2; 1^2$	393
256	2^2	8 948	822	7^2	40 900
294	1^4	4 073	826	$10^1; 1^2$	19 080
349	$3^1; 1^1$	2 956	853	$8^1; 5^1$	234
400	$4^1; 1^1$	1 539	853	$7^1; 1^6$	451
403	$2^2; 1^2$	855	875	14^1	19 020
411	7^1	180 900	892	$7^1; 6^1; 2^1$	5 415
442	1^6	909	907	$7^1; 3^1; 1^3$	566
480	$6^1; 2^1$	10 330	909	$4^2; 2^2$	290
496	$3^1; 1^3$	693	912	16^1	122 500
512	2^4	353	923	$7^1; 2^4$	186
547	$4^1; 1^3$	687	929	$12^1; 2^1$	1 908
550	3^2	2 836	935	$10^1; 2^2$	3 658
558	$7^1; 1^2$	15 040	945	$9^1; 3^1; 1^2$	823
597	$9^1; 1^1$	187	947	$4^2; 1^4$	288
601	$4^1; 3^1$	2 662	958	$7^1; 4^1; 1^3$	318
627	$6^1; 2^1; 1^2$	977	961	$6^2; 2^2$	383
643	$3^1; 1^5$	255	961	$7^1; 3^2$	2 062
653	4^2	11 080	970	$7^2; 1^2$	5 499
667	$7^1; 2^2$	4 741	973	$10^1; 1^4$	2 530
679	10^1	140 000	1013	$7^1; 4^1; 3^1$	1 330
697	$3^2; 1^2$	631	1022	$14^1; 1^2$	1 581
706	$7^1; 1^4$	3 026	1027	$10^1; 3^1; 1^1$	1 776
736	$6^1; 2^3$	814	1039	$7^1; 6^1; 2^1; 1^2$	444
760	$7^1; 3^1; 1^1$	1 279	1053	$4^3; 1^1$	234
798	$9^1; 3^1$	5 408	1059	$16^1; 1^2$	17 720
800	$4^2; 1^2$	1 067	1064	$7^1; 4^2$	4 773

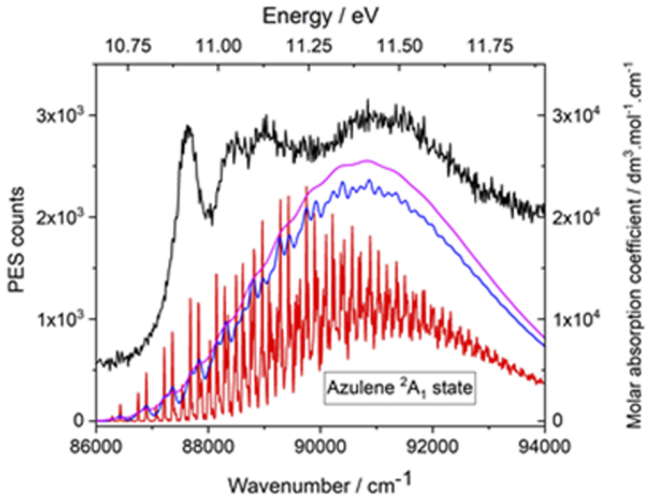

FIG. 8. Bands D and E. An overlapping set of peaks assigned to the 2^2B_1 and 1^2A_1 ionic states determined using the CAM-B3LYP method. The theoretical levels of 1^2A_1 are overlaid and show sets of vibrational peaks corresponding to half-widths at half-maximum of 10 cm^{-1} (red), 70 cm^{-1} (magenta), and 150 cm^{-1} (blue).

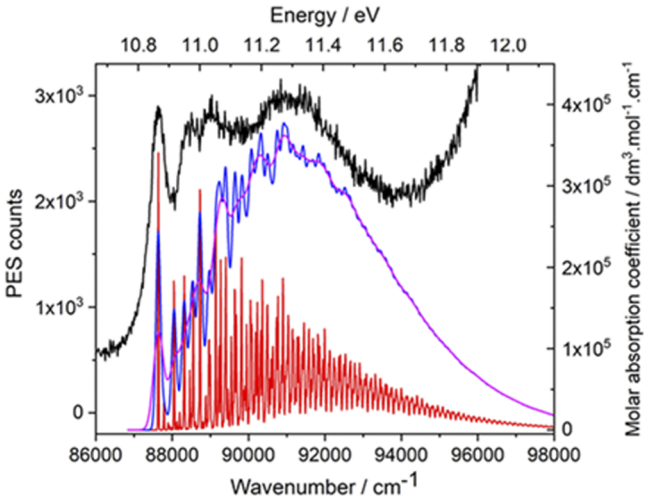

FIG. 9. Bands D and E. The theoretical levels of the 2^2B_1 state, determined by the CASSCF method, are overlaid to show sets of vibrational peaks corresponding to half-widths at half-maximum of 10 cm^{-1} (red), 70 cm^{-1} (magenta), and 150 cm^{-1} (blue).

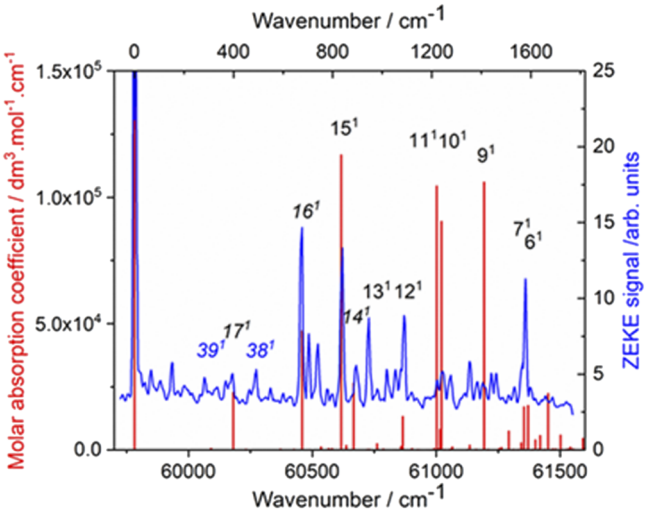

FIG. 10. The ZEKE electron spectrum of azulene obtained via the S2 origin (in blue), as reproduced with permission from Tanaka *et al*., Chem. Phys. **239**, 437–445 (1998). Copyright 1998 Elsevier. This is compared with the Franck–Condon profile for the 1^2A_2 state (in red), determined using the CAM-B3LYP method. Modes 39, 17, 38, 14, and 13 shown in italics are those proposed by Tanaka *et al.*;[16] the a_1 group of these is consistent with the Franck–Condon analysis given here. Non-italicized modes are based on the present study.

who chose the mode sequence: a_1 (ν_1 to ν_{17}), a_2 (ν_{18} to ν_{23}), b_1 (ν_{24} to ν_{39}), and b_2 (ν_{40} to ν_{48}), as noted above. This contrasts with the G-16 system, where b_1 has nine modes, while b_2 has 16 modes. However, for simplicity, we have adopted, for this section only, to follow Tanaka *et al.*[16] to avoid complications. They attributed the ZEKE series of vibrations above[16,43] to modes 39(b_1), 17(a_1), 38(b_1), 16(a_1), $17^2(a_1)$, $14^1(a_1)$, and $13^1(a_1)$, respectively. These are indicated in Fig. 10, where the a_1 modes from the present study are shown in black, with the two b_1 vibrations of Tanaka *et al.* shown in blue. Our calculated Franck–Condon vibrational frequencies for the 17, 16, 14, and 13 a_1 bands are in close agreement with their work. Further details of the procedure for re-generating the ZEKE spectrum are given in the supplementary material as SM7. Thus, we can interpolate the ZEKE spectrum with additional assignments as shown. Differences between the two studies have a maximum difference of 50 cm^{-1}, making these indistinguishable in Fig. 10.

Two ZEKE vibrations were attributed to non-symmetric modes, which must occur via vibronic coupling with another state.[16,43] The fluorescence excitation spectral study also led to the very small separation of ν_{16} (a_1, 662 cm^{-1}) from ν_{37} (b_1, 668 cm^{-1}). The observation of several b_1 vibrations in the ZEKE and other spectra probably comes from the vibronic coupling with the $S_3(^1B_1)$ state, which lies 5000 cm^{-1} above the S_2 state. That is, the S_2 state borrows absorption intensity by coupling with both the $S_4(^1A_1)$ and $S_3(^1B_1)$ states.[17]

Initially, the theoretical 1^2A_2 Franck–Condon line intensities, using the CAM-B3LYP harmonic frequency results, were corrected for the difference in 0–0 band positions, and the results scaled between the two spectra. We correlated the 17^1, 16^1, and 14^1 bands, between the two sets of data, since our results are in agreement with those of Takana *et al.*[16] The correlation line is $\nu_{Calc}^{ZEKE} = 0.9714 \times \nu_{Calc}^{FC} + 1711\ cm^{-1}$; thus, the whole theoretical spectrum has been shifted to higher energies by 1711 cm^{-1} (0.2121 eV); the energies are 97.1% of those measured experimentally. Overall, this is a very close correlation.

TABLE IX. The non-scaled and scaled CAM-B3LYP anharmonic frequencies made to correlate with the ZEKE spectral frequencies.

Estimated peak positions in ZEKE spectrum. 0–0 band intensity is 100 units					
Energy from 0 to 0 band (cm^{-1})	Relative local intensity/arbitrary units	Corrected[a] anharmonic calc. (cm^{-1})	Difference from ZEKE (cm^{-1})	Assignment G-16 ascending sequence	Standard a_1 assignment
394	2	387	7.0	6^1	17^1
671	21	674	−3.4	10^1	16^1
835	12	836	−0.8	15^1	15^1
886	3	887	−0.6	17^1	14^1
938	10	951	−12.6	19^1	13^1
1079	7	1094	−14.8	26^1	12^1
1245	2	1229	16.2		11^1
1271	2	1252	18.8		10^1
1411	2	1418	−6.7		9^1
		1481	⋯		8^1
1580	6	1583	−3.2	39^1	7^1
		1593	⋯		6^1

[a]The anharmonic frequencies are directly related to the ZEKE set by $\nu_{ZEKE} = 1.015 * \nu_{Anharmonic} - 25.314\ cm^{-1}$.

We performed a major expansion of the reported ZEKE spectrum,[16] as described in the supplementary material as SM7, to generate the much amplified blue line in Fig. 10. Some variations in the band intensities may have occurred during this process, but intensities are not central to the theme.

In a second phase, we used the corresponding CAM-B3LYP anharmonic frequency determinations at the Franck–Condon level for the theoretical 1^2A_2 state. These results are shown in Fig. 10 as a (red) stick diagram, superimposed on the (blue) ZEKE spectrum. Our data are shown in Table IX. An important conclusion is that the anharmonic calculations, using the same basis set and theoretical method for azulene, lead to a mean correction to fit the ZEKE data, which is reduced from 32.7 cm^{-1} for the harmonic frequencies to 11.1 cm^{-1} for the CAM-B3LYP anharmonic set. All the modes, marked in black in Fig. 10, are Franck–Condon modes and hence of a_1 symmetry. The b_1 modes of Tanaka *et al.*[16] are also labeled 38 and 39 (in blue). The a_1 modes shown suggest that the ZEKE spectrum can be provisionally subject to further assignment of vibrational states in the $^2A_2$ ionic state.

IV. CONCLUSIONS

Azulene is a historically important molecule both experimentally and theoretically. In this paper, we reinvestigate its photoelectron spectrum with a view of interpretation of the vibrational structure disclosed by the present synchrotron-based PES. The closely related ZEKE spectra fit closely into this study and are similarly analyzed.

The two lowest ionization bands of the PES (bands A and B) both show a range of vibrations, which have been interpreted by Franck–Condon methods for the first time; superficially similar in appearance, there are significant differences in the principal modes present. The third ionization band, band C, is comparatively narrow in comparison to A and B; this is a result of only lower frequency vibrations occurring in band C. The onset of the combined band D + E has the appearance of π-electron ionization, from its local high onset intensity and narrow width. The calculated sequence, however, shows that it is largely overlaid by the first σ-state, 1^2A_1. The greatly differing intensities of the 0–0 bands for these states enable a reasonable interpretation.

Above 11 eV, the PES shows a series of broadbands, each of which has the appearance of more than one ionization lying underneath. Our single excitation CI study is in almost exact agreement with our symmetry adapted coupled cluster study, using the SAC-CI code, for this whole spectrum of up to 19 eV. A number of shake-up states accompany the principal one-electron ionizations, but rather fewer than previously suggested.[41]

The previously reported ZEKE spectrum[16,43] is based on the 1^2A_2 ionic state, under band A of the PES. We have found that the both current triple-zeta with single polarization results not only agree with most of the previous interpretation but also offer an expansion of the number of modes present. The separations of our theoretical a_1 symmetry fundamental modes for the 1^2A_2 state from the 0–0 band match with those proposed by Tanaka *et al.*[16] for modes 17, 16, and 14. This enables us to superimpose the most prominent a_1 fundamentals upon the ZEKE spectrum and arrive at several new proposals for a_1 band positions. We are unable to offer an alternative explanation for any assignment based on non-symmetric vibrations since our analysis was performed under Franck–Condon conditions. This is not to deny the possibility of such vibrations being present, but we propose that a simpler interpretation is possible for several more a_1 mode assignments.

SUPPLEMENTARY MATERIAL

See the supplementary material for additional information on each of the following: The multi-peak analysis (SM1). The ground and ionic state structures (SM2). The MCSCF states (SM3). Tamm–Dancoff approximation (TDA) (SM4). Full sequences of harmonic frequencies for ionic states of azulene (SM5). Higher vibrational states from the 1^2A_1 Franck–Condon calculation, and these higher combination bands are where the principal intensity lies and cover the region up to the band maximum (SM6). Recovery of the ZEKE spectrum shown in Fig. 10 (SM7).

ACKNOWLEDGMENTS

We acknowledge the Elettra Synchrotron facility for the grant of beamtime. We thank C. Puglia (Uppsala University, Sweden) and acknowledge the Carl Tyggers Foundation for making available the VG-Scienta SES-200 photoelectron analyzer. We also acknowledge the University of Edinburgh (Eddie3) and Edinburgh Parallel Computing Center (Cirrus) super-computing facilities for support.

AUTHOR DECLARATIONS

Conflict of Interest

The authors have no conflicts of interest to declare.

DATA AVAILABILITY

The data that support the findings of this study are available within the article and its supplementary material and from the corresponding author upon reasonable request.

REFERENCES

[1] M. H. Palmer, M. Coreno, M. de Simone, C. Grazioli, S. V. Hoffmann, and N. C. Jones, J. Chem. Phys. **150**, 194305 (2019).
[2] M. H. Palmer, S. V. Hoffmann, N. C. Jones, M. Coreno, M. de Simone, and C. Grazioli, J. Chem. Phys. **151**, 084304 (2019).
[3] M. H. Palmer, R. A. Aitken, M. Coreno, M. de Simone, C. Grazioli, S. V. Hoffmann, and N. C. Jones, J. Chem. Phys. **152**, 144301 (2020).
[4] M. H. Palmer, S. V. Hoffmann, N. C. Jones, M. Coreno, M. de Simone, C. Grazioli, and R. A. Aitken, J. Chem. Phys. **153**, 054301 (2020).
[5] M. H. Palmer, M. Coreno, M. de Simone, C. Grazioli, R. A. Aitken, S. V. Hoffmann, N. C. Jones, and C. Peureux, J. Chem. Phys. **153**, 204303 (2020).
[6] M. H. Palmer, S. V. Hoffmann, N. C. Jones, M. Coreno, M. de Simone, C. Grazioli, and R. A. Aitken, J. Chem. Phys. **155**, 034308 (2021).
[7] H. H. Jaffe and M. Orchin, in *Theory and Applications of Ultraviolet Spectroscopy* (Wiley, New York, 1962), Chap. 13.9, pp. 337–344.

[8]R. G. Parr, *The Quantum Theory of Molecular Electronic Structure* (Benjamin, New York, 1964), p. 58.
[9]G. M. Badger, *Aromatic Character and Aromaticity*, Cambridge Texts in Chemistry and Biochemistry (Cambridge University Press, 1969), ISBN: 9780521095433.
[10]L. Salem, in *The Molecular Orbital Theory of Conjugated Systems* (W. A. Benjamin, New York, 1966), Chaps. 1–5 and 1–6.
[11]J. H. D. Eland and C. J. Danby, Z. Naturforsch. A **23**, 355–357 (1968).
[12]R. Boschi, E. Clar, and W. Schmidt, J. Chem. Phys. **60**, 4406–4418 (1974).
[13]P. M. Weber and N. Thantu, Chem. Phys. Lett. **197**, 556–561 (1992).
[14]H. J. Tobler, A. Bauder, and H. H. Günthard, J. Mol. Spectrosc. **18**, 239–246 (1965).
[15]S. Huber, G. Grassi, and A. Bauder, Mol. Phys. **103**, 1395–1409 (2005); S. Thorwirth, P. Theule, C. A. Gottlieb, M. C. McCarthy, and P. Thaddeus, Astrophys. J. **662**, 1309–1314 (2007).
[16]D. Tanaka, S. Sato, and K. Kimura, Chem. Phys. **239**, 437–445 (1998).
[17]M. Fujii, T. Ebata, N. Mikami, and M. Ito, Chem. Phys. **77**, 191–200 (1983).
[18]R. S. Chao and R. K. Khanna, Spectrochim. Acta, Part A **33**, 53–62 (1977).
[19]V. Barone, J. Bloino, M. Biczysko, and F. Santoro, J. Chem. Theory Comput. **5**, 540–554 (2009).
[20]J. Bloino, M. Biczysko, F. Santoro, and V. Barone, J. Chem. Theory Comput. **6**, 1256–1274 (2010).
[21]A. Baiardi, J. Bloino, and V. Barone, J. Chem. Theory Comput. **9**, 4097–4115 (2013).
[22]M. J. Frisch, G. W. Trucks, H. B. Schlegel, G. E. Scuseria, M. A. Robb, J. R. Cheeseman, G. Scalmani, V. Barone, G. A. Petersson, H. Nakatsuji, X. Li, M. Caricato, A. V. Marenich, J. Bloino, B. G. Janesko, R. Gomperts, B. Mennucci, H. P. Hratchian, J. V. Ortiz, A. F. Izmaylov, J. L. Sonnenberg, D. Williams-Young, F. Ding, F. Lipparini, F. Egidi, J. Goings, B. Peng, A. Petrone, T. Henderson, D. Ranasinghe, V. G. Zakrzewski, J. Gao, N. Rega, G. Zheng, W. Liang, M. Hada, M. Ehara, K. Toyota, R. Fukuda, J. Hasegawa, M. Ishida, T. Nakajima, Y. Honda, O. Kitao, H. Nakai, T. Vreven, K. Throssell, J. A. Montgomery, Jr., J. E. Peralta, F. Ogliaro, M. J. Bearpark, J. J. Heyd, E. N. Brothers, K. N. Kudin, V. N. Staroverov, T. A. Keith, R. Kobayashi, J. Normand, K. Raghavachari, A. P. Rendell, J. C. Burant, S. S. Iyengar, J. Tomasi, M. Cossi, J. M. Millam, M. Klene, C. Adamo, R. Cammi, J. W. Ochterski, R. L. Martin, K. Morokuma, O. Farkas, J. B. Foresman, and D. J. Fox, Gaussian 16, Revision A.03, Gaussian, Inc., Wallingford, CT, 2016.
[23]R. G. Parr and W. Yang, *Density-Functional Theory of Atoms and Molecules* (Oxford University Press, Oxford, 1989).
[24]A. D. Becke, J. Chem. Phys. **98**, 5648–5652 (1993).
[25]T. Yanai, D. P. Tew, and N. C. Handy, Chem. Phys. Lett. **393**, 51–57 (2004).
[26]S. Grimme, J. Chem. Phys. **124**, 034108 (2006).
[27]S. Grimme, S. Ehrlich, and L. Goerigk, J. Comput. Chem. **32**, 1456–1465 (2011).
[28]T. Schwabe and S. Grimme, Phys. Chem. Chem. Phys. **9**, 3397–3406 (2007).
[29]H.-J. Werner, P. J. Knowles, F. R. Manby, M. Schütz, P. Celani, T. Korona, R. Lindh, A. Mitrushenkov, G. Rauhut, K. R. Shamasundar, T. B. Adler, R. D. Amos, A. Bernhardsson, A. Berning, D. L. Cooper, M. J. O. Deegan, A. J. Dobbyn, F. Eckert, E. Goll, C. Hampel, A. Hesselmann, G. Hetzer, T. Hrenar, G. Jansen, C. Köppl, Y. Liu, A. W. Lloyd, R. A. Mata, A. J. May, S. J. McNicholas, W. Meyer, M. E. Mura, A. Nicklaß, D. P. O'Neill, P. Palmieri, K. Pflüger, R. Pitzer, M. Reiher, T. Shiozaki, H. Stoll, A. J. Stone, R. Tarroni, T. Thorsteinsson, M. Wang, and A. Wolf, MOLPRO, version 2012.1, a package of *ab initio* programs, 2012, see http://www.molpro.net.
[30]R. Ahlrichs and P. R. Taylor, J. Chim. Phys. **78**, 315–324 (1981).
[31]A. Schaefer, H. Horn, and R. Ahlrichs, J. Chem. Phys. **97**, 2571–2577 (1992).
[32]H. Nakatsuji and K. Hirao, Int. J. Quantum Chem. **20**, 1301–1313 (1981).
[33]H. Nakatsuji and T. Yonezawa, Chem. Phys. Lett. **87**, 426–431 (1982).
[34]H. Nakatsuji, Chem. Phys. **75**, 425–441 (1983).
[35]H. Nakatsuji, Int. J. Quantum Chem. **24**(S17), 241–255 (1983).
[36]H. Nakatsuji, K. Ohta, and T. Yonezawa, J. Phys. Chem. **87**, 3068–3074 (1983).
[37]W. von Niessen, L. S. Cederbaum, and W. P. Kraemer, J. Chem. Phys. **65**, 1378–1386 (1976).
[38]L. S. Cederbaum and W. Domcke, in *Advance in Chemical Physics*, edited by I. Prigogine and S. A. Rice (Wiley and Sons, Inc., 1977), Vol. XXXVI, pp. 205–344.
[39]W. von Neissen, J. Schirmer, and L. S. Cederbaum, Comput. Phys. Rep. **1**, 57–125 (1984).
[40]M. F. Guest, I. J. Bush, H. J. J. Van Dam, P. Sherwood, J. M. H. Thomas, J. H. Van Lenthe, R. W. A. Havenith, and J. Kendrick, Mol. Phys. **103**, 719–747 (2005).
[41]M. S. Deleuze, J. Chem. Phys. **116**, 7012–7026 (2002).
[42]R. J. Buenker and S. D. Peyerimhoff, Chem. Phys. Lett. **3**, 37–42 (1969).
[43]K. Kimura, J. Electron Spectrosc. Relat. Phenom. **100**, 273–296 (1999).